

## Adsorption Dynamics for the Capillary Condensation of Trichloroethylene Vapor on Mesoporous Material

Wang Geun Shim, Jae Wook Lee\*, Hyun-Ku Rhee\*\* and Hee Moon<sup>†</sup>

Faculty of Applied Chemistry, Chonnam National University, Gwangju 500-757, Korea

\*Department of Chemical Engineering, Seonam University, Namwon 590-711, Korea

\*\*School of Chemical Engineering, Seoul National University, Seoul 151-742, Korea

(Received 31 October 2003 • accepted 15 January 2004)

**Abstract**—The adsorption of Trichloroethylene (TCE) vapors on both powder and pelletized MCM-48 was measured by using a quartz spring balance equipped in a high vacuum system. Single species equilibrium data show typical IV isotherms based on the IUPAC classification. Equilibrium data obtained were reasonably well fitted to a temperature-dependent hybrid (Langmuir+Sips) isotherm. To investigate the applicability of the hybrid isotherm on the prediction of breakthrough patterns, experimental and theoretical studies were carried out in a fixed bed charged with MCM-48.

Key words: Adsorption, Fixed Bed, Hybrid Isotherm, MCM-48, Trichloroethylene

### INTRODUCTION

Chlorinated volatile organic compounds (CVOC) have been produced commercially and used for many purposes in industries. Trichloroethylene (TCE) is widely used as a degreasing agent in five main industrial groups: furniture and fixtures, fabricated metal products, electrical and electronic equipment, transport equipment, and miscellaneous manufacturing industries. The primary releases of TCE are from degreasing operations and industrial wastewater streams. According to the 9<sup>th</sup> report on carcinogens, TCE is reasonably anticipated to be a carcinogenic substance. Therefore, TCE is regulated under the EPA, FDA and other agencies [U.S. Department of Health and Human Services, 2001].

Due to the significant economic and environmental implications of disposing of CVOC, much attention has been recently directed towards cost-effective pollution prevention techniques aimed at reducing CVOC emissions from industrial facilities. The many techniques available to control CVOC emissions have different advantages and limitations. These techniques are basically classified into two different groups: destruction based and recovery based. In a practical CVOC removal process, an ideal adsorbent is expected to have (1) a large amount of reversible adsorption capacity (large accessible pore volume), (2) no catalytic activity, (3) hydrophobicity, (4) high thermal and hydrothermal stability, and (5) an easy regeneration property [Ruddy and Carroll, 1993; Khan and Ghoshal, 2000].

One of the most effective methods for controlling CVOC is an adsorption process. The main advantages of adsorption as compared with other separation techniques are its higher selectivity and relatively higher capacity for CVOC, even at low partial pressures. In general, it has been recognized that activated carbon is the most suitable adsorbent for this application. However, there are number

of problems associated with activated carbons such as combustion at high temperature, pore blocking, and hygroscopic property. To overcome these problems, various alternative adsorbents have been developed [Khan and Ghoshal, 2000; Kim et al., 2002; Cho et al., 2003].

A new family of ordered mesoporous materials, M41S, was developed by Mobil scientists in 1992. Characteristic properties of these materials are large surface area and narrow pore size distribution. There are well-defined porous adsorbents in the family of M41S materials. MCM-41 has a hexagonal arrangement of unidirectional pores while MCM-48 has a cubic structure indexed in the space group. While nitrogen adsorption data are published in almost every paper dealing with the M41S family of materials, studies on adsorption of organics in MCM-41 and MCM-48 are very limited [Corra, 1997; Lee et al., 2003]. In practical applications, the mechanical stability is an important characteristic of an adsorbent. Recently, Hartmann and Bischof [1999] investigated the mechanical stability of the silica mesoporous MCM-48 using powder X-ray diffraction, nitrogen adsorption, subcritical organic vapor, adsorption isotherms, and experimental breakthrough curves.

Fixed bed adsorption has been an important unit operation for separation and purification in engineering applications. The adsorber dynamics in general depends on several factors such as bed geometry, adsorption system, operating conditions, heat and kinetic effects, and adsorption equilibrium relationships. Especially, it has been realized that the shape of the equilibrium isotherm greatly influences adsorber dynamics. Park and Knabel [1992] studied an adsorption system of water vapor and silica gel, which exhibits type IV isotherm. According to their results, the equilibrium isotherm and heat effects can cause unusual dynamics in fixed bed adsorbents. Recently, Yun [1997] investigated the unusual adsorber dynamics for S-shaped equilibrium isotherms of solvent vapors on a dealuminated zeolite Y. He suggested that the basic shape of the adsorption isotherm influences the unusual column dynamics. In general, adsorption isotherms of VOC vapors on mesoporous adsorbents, unlike other type IV adsorption equilibrium isotherms, show a highly sharp increase

<sup>†</sup>To whom correspondence should be addressed.

E-mail: hmoon@chonnam.ac.kr

<sup>‡</sup>This paper is dedicated to Professor Hyun-Ku Rhee on the occasion of his retirement from Seoul National University.

in a certain relative pressure [Hartmann and Bischof, 1999; Zhao et al., 2001; Shim et al., 2001]. However, there are no general adsorption isotherm models to correlate the adsorption equilibrium data. Furthermore, it is not easy to find a fixed bed dynamics for gaseous vapors on mesoporous adsorbents, except a report by Hartmann and Bischof [1999]. Therefore, it is important to study adsorption equilibrium and fixed bed breakthrough behavior with a quantitative analysis.

In this work, an interesting dynamic behavior of TCE was studied for the MCM-48. The MCM-48/TCE adsorption system shows remarkable capillary condensation and highly unusual adsorption breakthrough patterns. To investigate the effect of adsorption isotherm on the breakthrough patterns systematically, both experimental and theoretical studies were done in a fixed bed charged with manufactured MCM-48. The adsorption of TCE vapors on both powder and pelletized MCM-48 was measured accurately by using a quartz spring balance. To correlate the single species adsorption equilibrium data, a temperature-dependent hybrid (Langmuir+Sips) isotherm was proposed [Lee et al., 2003; Oh et al., 2003]. Also, a simple adsorption dynamic model was developed by employing the mass balances both in the gas and solid phases, and the mass transfer resistance through the adsorbent.

## EXPERIMENTAL

### 1. Material Preparation and Characterization

MCM-48 sample was synthesized as follows. 12.4 g of cetyltrimethylammonium bromide (CTMABr,  $C_{19}H_{42}BrN$ , Aldrich), 2.16 g LE-4 (polyoxyethylene lauryl ether,  $C_{12}H_{25}(OCH_2CH_2)_4OH$ , Aldrich) were dissolved in a Teflon bottle containing 130 g of deionized water at 333 K. This aqueous solution was added dropwise to another aqueous solution in the Teflon bottle containing 40 g of Ludox AS-40 (Du Pont, 40 wt% colloidal silica in water), 5 g of NaOH, and 130 g of deionized water under vigorous stirring. The solution mixture was preheated in a water bath kept at 313 K and was stirred at 500 rpm for 20 min. The resultant gel was loaded to an autoclave, and the mixture was hydrothermally treated at 373 K for 78 h. The mixture was then filtered and washed with 500 mL deionized water. The washing procedure was repeated 4-5 times to ensure the complete removal of bromide and other free ions. After drying at 333 K for overnight, the dried solid was then calcined in air at 873 K for 10 h.

To test the adsorption property of MCM-48, the samples were compressed by using a hand-operated press. The pelletized MCM-48 diameter is 10 mm and the external pressure applied is 200 kg/cm<sup>2</sup>. Subsequently, the obtained pellet was crushed and sieved to obtain pellets with a diameter of 1.0 to 2.0 mm that were used for adsorption equilibrium and fixed bed studies.

In designing an adsorption column, the characterization of adsorbents should be done prior to experiments. In particular, one should know not only the specific area but also the pore size distribution of the adsorbent in order to confirm that it would be proper for the given purpose. The surface area and pore volumes of MCM-48 measured by using a Micrometrics ASAP 2000 automatic analyzer are listed in Table 1. X-ray powder diffraction data of mesoporous sorbents were collected on a Phillips PW3123 diffractometer equipped with a graphite monochromator and Cu K $\alpha$  radiation of wavelength

**Table 1. The physical properties of the particles**

Property	Powder	Pellet	Unit
Particle size	$7.0 \times 10^{-7}$	$1.5 \times 10^{-3}$	m
Packing density	240	350	kg/m <sup>3</sup>
Surface area	990	850	m <sup>2</sup>
Mean pore size	32	32	Å

0.154 nm. XRD patterns were obtained between 2° and 50° with a scan speed of 1°/min.

### 2. Gravimetric Apparatus

The adsorption amount of TCE vapor was measured by a quartz spring balance, which was placed in a closed glass system. A given amount of carbon particles were placed on the dish, which was attached to the end of quartz spring [Lee et al., 2003; Shim et al., 2003a]. This system was vacuumed for 15 hours at  $10^{-3}$  Pa and 250 °C to remove volatile impurities from the MCM-48 particles. A turbomolecular pump (Edward type EXT70) in combination with a rotary vacuum pump (Edward model RV5) was used to evacuate the system. Pirani and penning vacuum gauges (Edwards Series 1000) were used for the measurement of vacuum. The pressure of the system was measured with a Baratron absolute pressure transducer (MKS instruments type 128) and a power supply read out instrument (Type PDR-C-1C). The variation of weight was measured by a digital voltmeter that was connected to the spring sensor. The adsorption equilibrium was usually attained within 30-60 min. Equilibrium experiments were carried out at four different temperatures of 303.15, 308.15 (powder), 313.15, and 323.15 K respectively.

### 3. Fixed Bed Apparatus

A schematic diagram of the fixed bed experimental setup is presented in Fig. 1. The physical properties of bed characteristics are given in Table 2. The apparatus was constructed with stainless steel tubes. It had three major sections: 1) apparatus for preparation of

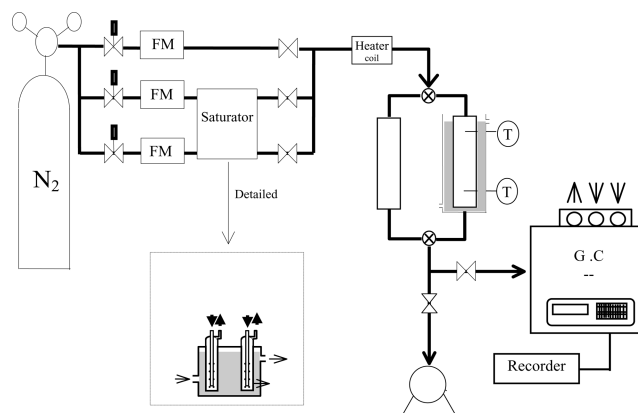


**Fig. 1. Experimental setup used for breakthrough experiments.**

**Table 2. Adsorption bed characteristics**

Property	Powder	Pellet	Unit
Length	$1.76 \times 10^{-1}$	$1.02 \times 10^{-1}$	m
Velocity	$3.89 \times 10^{-2}$	$5.52 \times 10^{-2}$	m/s
Column I.D.	1.0		cm
Temp	303.15		K

vapors, 2) adsorption column in a water bath, and 3) apparatus for the analysis of gas. The gas flow line of nitrogen was divided into three branches: one was for pure nitrogen gas and the other two were connected to solvent saturators. The concentration of each solvent was evaluated from its saturated vapor pressure at a given temperature by assuming its vapor-liquid equilibrium state. All lines were sufficiently heated (more than water bath) to prevent the saturated solvent vapors from condensing in the steel tubes. The gas mixture of saturated solvent vapors and pure nitrogen gas was delivered to the adsorption section. The gas flow through the column was controlled by mass flow controllers with a read-out power supply which was precalibrated against a soap bubble flow meter covering a wide range of flow rates under experimental pressures. The gas mixture was heated to the experimental temperature in the preheating section before being charged to the fixed-bed adsorber. Two K-type thermocouples were installed at inlet and outlet sections of the packed column, and the temperatures were monitored continuously on a display recorder. The composition of exit gas stream from the adsorption section was determined with a gas chromatographer, GC-14B model (Shimadzu), equipped with a hydrogen flame ionization detector. Helium was used as a carrier gas.

## THEORETICAL APPROACH

### 1. Fixed Bed Adsorption

In order to study the adsorption behavior of TCE in a fixed-bed adsorber, a dynamic model was developed. The adsorption system considered is an isothermal column packed with MCM-48, through which an inert gas flows at a steady state. This model includes the nonlinear adsorption isotherm, the mass balance in the gas and solid phases, the mass transfer resistance through the adsorbent. The model adopted here utilizes the hybrid isotherm equation and a linear driving force (LDF) rate model to simplify the diffusional mass transfer inside adsorbent particles. The LDF model is a lumped-parameter model for particle adsorption.

A simple model for an isothermal adsorption in a fixed bed is as follows:

Mass balance:

$$-D_L \frac{\partial^2 c}{\partial z^2} + v \frac{\partial c}{\partial z} + \frac{\partial c}{\partial t} + \frac{1-\varepsilon_B}{\varepsilon_B} \rho_s \frac{\partial q}{\partial t} = 0 \quad (1)$$

where  $D_L$  is the axial dispersion coefficient,  $v$  is the interstitial velocity,  $\varepsilon_B$  is the bed voidage, and  $\rho_s$  is the particle density.

The boundary conditions are:

$$D_L \left. \frac{\partial c}{\partial z} \right|_{z=0} = -v(c|_{z=0} - c|_{z=0}) \quad (2)$$

$$\left. \frac{\partial c}{\partial z} \right|_{z=L} = 0 \quad (3)$$

The associated initial conditions are:

$$c(z, 0) = c_0; \quad q(z, 0) = 0 \quad (7)$$

The mass-transfer rate inside particles can be represented by

$$\frac{\partial q}{\partial t} = k_s \cdot (q^* - q) \quad (8)$$

where  $k_s$  is the effective mass transfer coefficient, and  $q^*$  is the equilibrium adsorbed phase concentration.

The hybrid (Langmuir+Sips) equation was used for adsorption equilibrium prediction

$$q^* = q_m \left( \frac{b_1 c}{1 + b_1 c} + \frac{b_2 c^n}{1 + b_1 c^n} \right) \quad (9)$$

The temperature dependency values are as follows:

$$b_1 = b_{10} \exp \left[ -\frac{A}{R} \left( \frac{1}{T} - \frac{1}{T_{ref}} \right) \right] \quad (10)$$

$$b_2 = b_{20} \exp \left[ -\frac{B}{R} \left( \frac{1}{T} - \frac{1}{T_{ref}} \right) \right] \quad (11)$$

$$n = n_0 \exp \left[ -\frac{C}{R} \left( \frac{1}{T} - \frac{1}{T_{ref}} \right) \right] \quad (12)$$

where  $q_m$ ,  $b_1$ ,  $b_2$ , and  $n$  are the hybrid isotherm constants.

### 2. Estimation of Model Parameters from Experimental Curves

Analyzing or designing an adsorption process requires accurate kinetic information. There are essentially three consecutive mass transport steps associated with the adsorption of adsorbates by porous adsorbents.

The external mass-transfer coefficient,  $k_s$ , can be estimated from some correlations reported in literature. Among those correlations, the equation proposed by Wakao and Funazkri [1978] has been widely used for column adsorptions.

$$Sh = 2.0 + 1.1 Sc^{1/3} Re^{0.6} \quad (13)$$

The molecular diffusivity,  $D_m$ , was calculated by using the Fuller equation [1965]. The axial dispersion coefficient included in the model was calculated from the following equation [Edwards and Richardson, 1968]

$$\frac{1}{Pe} = \frac{0.73 \varepsilon_B}{Re Sc} + \frac{1}{2.0 \left( 1 + \frac{(13.0) \cdot (0.73) \cdot \varepsilon_B}{Re Sc} \right)} \quad (14)$$

The overall effective linear driving force rate constants for the experimental were estimated from the following correlation [Faroq and Ruthven, 1990]:

$$\frac{1}{k_s} = \frac{R_p q^* \rho_s}{3 k_f c_o} + \frac{R_p^2 q^* \rho_s}{15 \varepsilon_p D_e c_o} \quad (15)$$

which considers macropore and film resistances to the mass transfer. The mass transfer coefficient,  $k_s$ , was found by fitting the simulation breakthrough curves to experimental data [Malek and Faroq, 1997; Silva and Rodrigues, 1997; Hwang et al., 1997; Shim et al., 2003b].

### 3. Method of Solution - Numerical Solutions

The set of coupled parabolic second-order partial differential equations cannot be solved analytically. The preferred means of numerically solving this complicated set of partial differential equations is by using the orthogonal collocation method (OCM) to discretize the equations [Villadsen and Stewart, 1967]. The partial differential equations were reduced to a set of ordinary differential equations (ODEs) by this technique. The discretization was done for the spatial variable, resulting in a set of time derivative ODEs for the sorbate concentration. The resulting sets of ODEs were solved

by using the subroutine DVODE [Brown et al., 1989].

## RESULTS AND DISCUSSION

### 1. Adsorption Isotherm

Many equilibrium isotherm models have been proposed over the years. Some of these models have gained more importance than other models due to their simplicity and easy applicability [Malek and Farooq, 1997; Yang, 1987]. However, few isotherms have been developed for the adsorption-condensation of condensable vapors on porous adsorbents [Gregg and Sing, 1982; Sircar, 1987].

Figs. 2 and 3 show the adsorption isotherm of TCE on both pow-

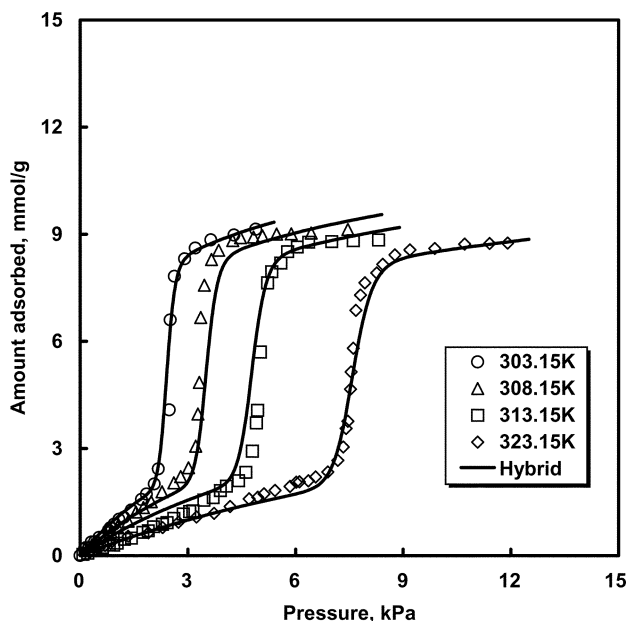


Fig. 2. Adsorption isotherms of TCE in powders of MCM-48.

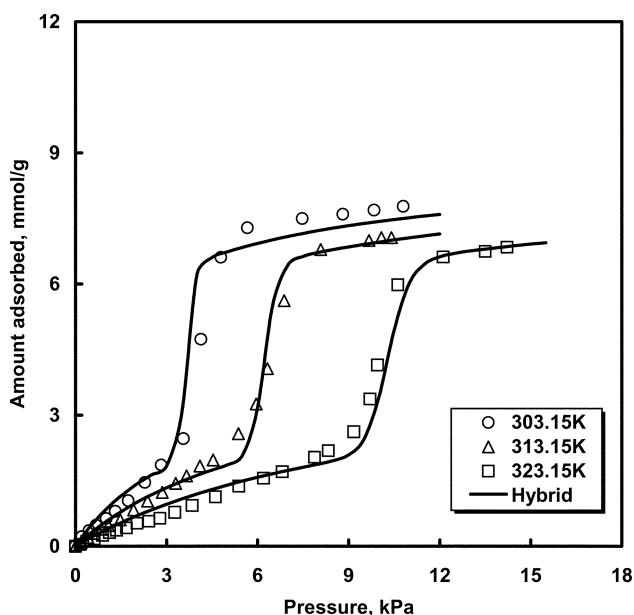


Fig. 3. Adsorption isotherms of TCE in pellets of MCM-48.

der and pelletized MCM-48 at various temperatures. The shape of isotherm on these materials shows complicated equilibrium relationships, which are distinguishable as linear and favorable types. The isotherms are type IV according to the IUPAC classification, with a steep increase between 0.2 and 0.3 in the powder type and between 0.3 and 0.4 in the pellet type relative pressures. The capillary condensation was observed at around  $P/P_0=0.20$  in the powder and at around  $P/P_0=0.30$  in the pellet. The last linear part of this isotherm is due to adsorption on the outer surface of particles and interparticle voids.

In the design of the adsorption process, practical engineering correlations for adsorption equilibrium are very important since the shape of the equilibrium isotherm greatly influences the adsorber dynamics. As it was hard to find any proper isotherm for the whole pressure region, the temperature-dependent hybrid isotherm was used. To find the isotherm parameters for each adsorption, the equations were determined by using a pattern search algorithm, namely the "Nelder-Mead simplex method" [Riggs, 1988]. The comparison of fit of data by the models was based on the square of residuals (SOR), defined as follows:

$$SOR = \frac{1}{2} \sum (q_{exp} - q_{cal})^2 \quad (13)$$

The SOR is an absolute value, the magnitude of which is dependent on the accuracy of fit as well as the number of experimental data [Malek and Farooq, 1997]. The hybrid isotherm model for a pure adsorbate was found to fit the individual isotherm data very well. The parameters of the hybrid equations are listed in Table 3.

As a useful thermodynamic property, the isosteric heat of adsorption has been generally applied to characterize the adsorbent surface. The isosteric heat of adsorption is evaluated simply by applying the Clausius-Clapeyron equation if one has a good set of adsorption equilibrium data obtained at several temperatures [Hill, 1949; Gregg and Sing, 1982].

$$\frac{q_{st}}{RT^2} = \left[ \frac{\partial \ln P}{\partial T} \right]_q \quad (14)$$

where  $q_{st}$  is the isosteric heat of adsorption,  $R$  is the gas constant, and  $q$  is the moles adsorbed. In Fig. 4, the isosteric heats of adsorption of vapors on both powdered and pelletized forms of MCM-48 are plotted as a function of the moles adsorbed. Because of the joint effects of the energetic non-uniformity of the adsorbent surface and the interaction of adsorbate molecules in the adsorbed film itself, the heat of adsorption in general varies significantly with the amount

Table 3. Hybrid equation parameters

	Powder	Pellet
$q_m$	6.116	4.357
$b_1$	$1.14 \times 10^{-1} \cdot \exp\left(\frac{46933}{RT}\right)$	$1.48 \times 10^{-1} \cdot \exp\left(\frac{37892}{RT}\right)$
$b_2$	$1.67 \times 10^{-17} \cdot \exp\left(\frac{1562843}{RT}\right)$	$1.11 \times 10^{-23} \cdot \exp\left(\frac{1224384}{RT}\right)$
$n$	$2.47 \times 10^1 \cdot \exp\left(-\frac{11340}{RT}\right)$	$2.89 \times 10^1 \cdot \exp\left(-\frac{1.822}{RT}\right)$
SOR	29.006 (NE=132)	1.019 (NE=59)

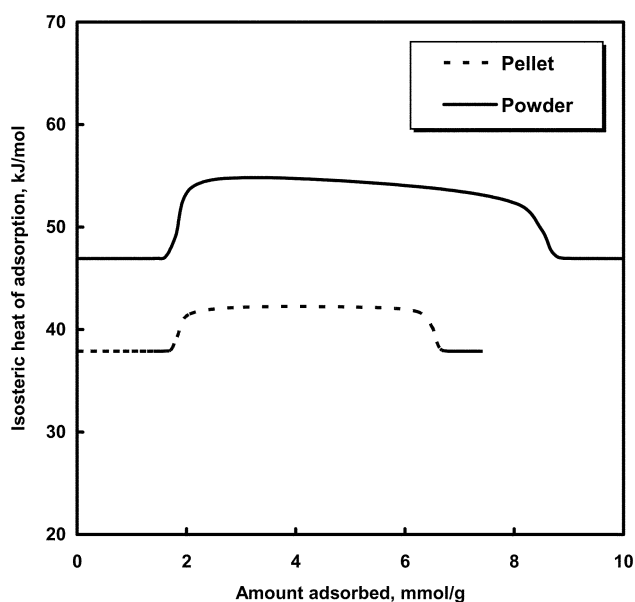


Fig. 4. Isosteric heat of adsorption as a function of the moles adsorbed.

adsorbed. The isosteric heat of adsorption can be divided into two sections, namely, in low concentration and capillary condensation regions. Especially, in the capillary condensation range, the isosteric heat of adsorption changes rapidly. It supports that bonding among TCE molecules in the condensed phase and between adsorbed layer and MCM-48 surfaces plays a key role in determining the desorption characteristics because the isosteric heat of adsorption is considered as the isosteric heat of desorption. In Fig. 4, the order of magnitude for  $q_m$  is powder > pellet. From the above results, the MCM-48 surface is heterogeneous, and this heterogeneity may come from structural heterogeneity because the capillary condensation is highly sensitive to the structure properties of pore size and pore distribution.

## 2. Fixed-bed Adsorption

The performance of an adsorption-based process greatly depends upon the effectiveness of design and operating conditions. Therefore, rigorous approaches to the design and operation of the adsorption system must be used to ensure efficient applications. To do this, one has to understand the mechanism and dynamics of adsorption and desorption, as well as major variables that affect the process performance. In this study, breakthrough experiments of TCE in MCM-48 powder and MCM-48 pellet beds were performed at various concentrations.

### 2-1. Results of the Adsorption Isotherm Parameter Sensitivity

Before verifying the experimental results, we tested the effects of adsorption isotherm parameters  $q_m$ ,  $b_1$ ,  $b_2$ , and  $n$ . Figs. 5 and 6 shows the exit concentration profiles obtained by using different values of  $q_m$ ,  $b_1$ ,  $b_2$ , and  $n$ . The equilibrium model parameters used in this run are the hybrid isotherm parameters for TCE adsorption on MCM-48 pellet. It is to be noted that the length of the concentration plateau zone becomes longer for a higher value of  $q_m$  and this value affects the whole concentration region. The parameter  $b_1$  that is related to the Langmuir isotherm region greatly affects the low concentration region before the effluent concentration profile reaches a plateau. The parameters  $b_2$  and  $n$ , which are related to the

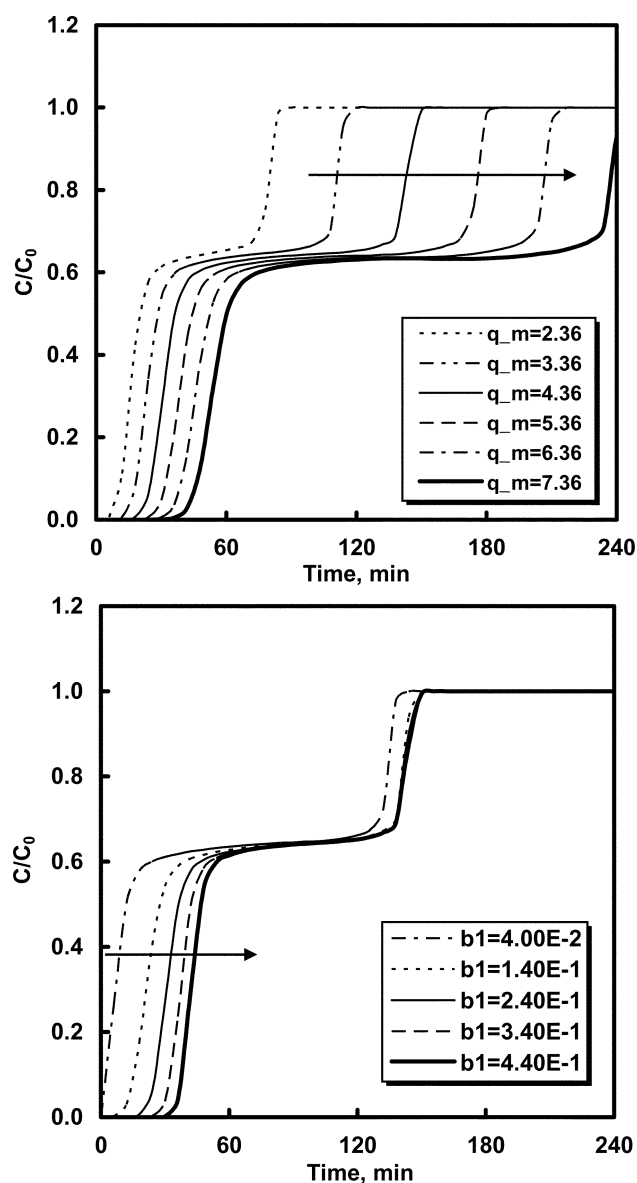


Fig. 5. Effect of temperature dependent parameter  $q_m$ ,  $b_1$  on the concentration breakthrough profiles.

Sips isotherm region, however, significantly affect the whole region. Especially, the length of plateau depends on the  $b_2$  and  $n$ .

One can conclude that the hybrid isotherm has two regions. The first is a linear or favorable region that depends on the Langmuir isotherm parameter, and the Sips isotherm parameter, which greatly affects the capillary condensation region.

### 2-2. Comparison with the Experimental Results

To investigate the influence of adsorption isotherm shape on breakthrough behavior, several fixed bed experiments were performed under the conditions of various influent TCE concentrations. The adsorption breakthrough curve of TCE over the powdered MCM-48 adsorbent is shown in Fig. 7. The experimental results obtained here show that the concentration breakthrough curve reached a plateau at about  $C/C_0=0.6$ . The plateau, which is related to the capillary condensation, was maintained for about 500 min. The length of this plateau is closely connected with the essential time to achieve

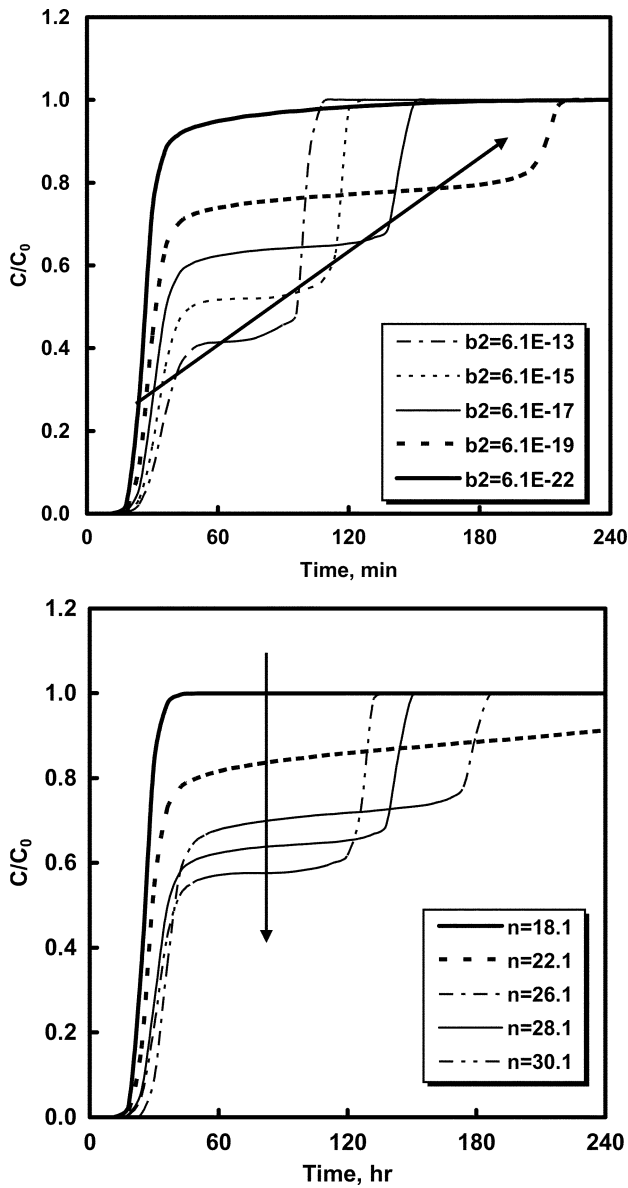


Fig. 6. Effect of temperature dependent parameter  $b_2$ ,  $n$  on the concentration breakthrough profiles.

a complete pore filling. Typical experimental adsorption breakthrough curves with the model simulation results for the MCM-48 pelletized are illustrated in Fig. 8. A good agreement between experimental and simulated results can be observed. In this system, the breakthrough patterns were strongly influenced by the inlet TCE concentrations. When the adsorption isotherm has an inflection point (Figs. 2 and 3), it represents a combination of favorable (low concentration) and unfavorable (high concentration) patterns. In the case of low TCE concentration ranges, the effluent concentration profile showed a typical proportional pattern. In the case of relatively high TCE concentration ranges, however, the effluent concentration profile reached a plateau. The obtained mass transfer coefficient for capillary condensation region ( $0.005 \text{ s}^{-1}$ ) is less than that for inter surface adsorption region ( $0.009 \text{ s}^{-1}$ ) [Lee et al., submitted].

Fig. 9 shows the theoretical concentration profiles in the bed for

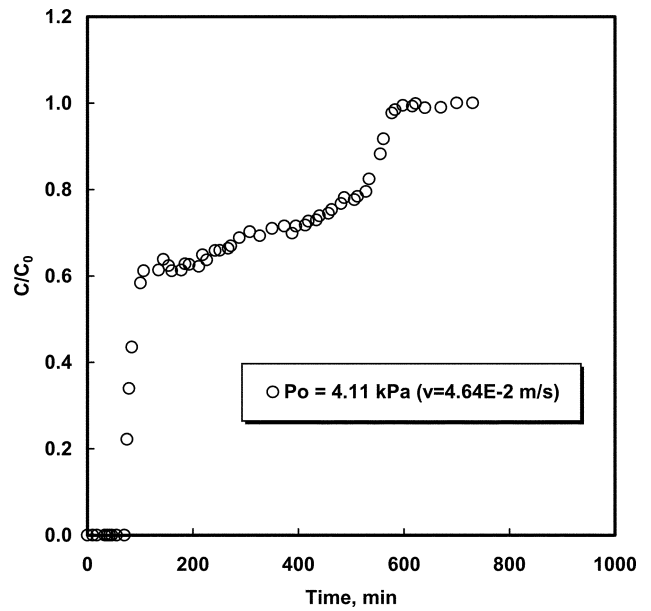


Fig. 7. Adsorption breakthrough curves of TCE on MCM-48 powder.

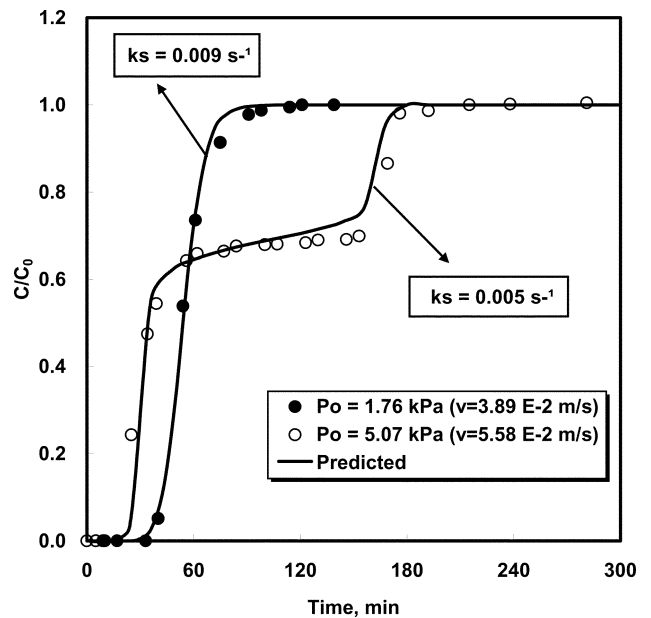


Fig. 8. Comparison of experimental and theoretical breakthrough curves of TCE on MCM-48 pellet.

the favorable and capillary condensation regions. In the low concentration region (1.76 kPa), the propagation profile tends to exhibit a constant pattern along the bed at early stages, but the profile slowly becomes broader as the concentration front moves toward the outlet at a steady velocity. At the capillary condensation region (5.07 kPa), the concentration profile starts with initial pattern similar to that of favorable region; however, it evolves to a shock wave that expands through the higher concentration range, instead of maintaining a proportional pattern.

2-3. Desorption

In practical processes, the desorption step would be as important

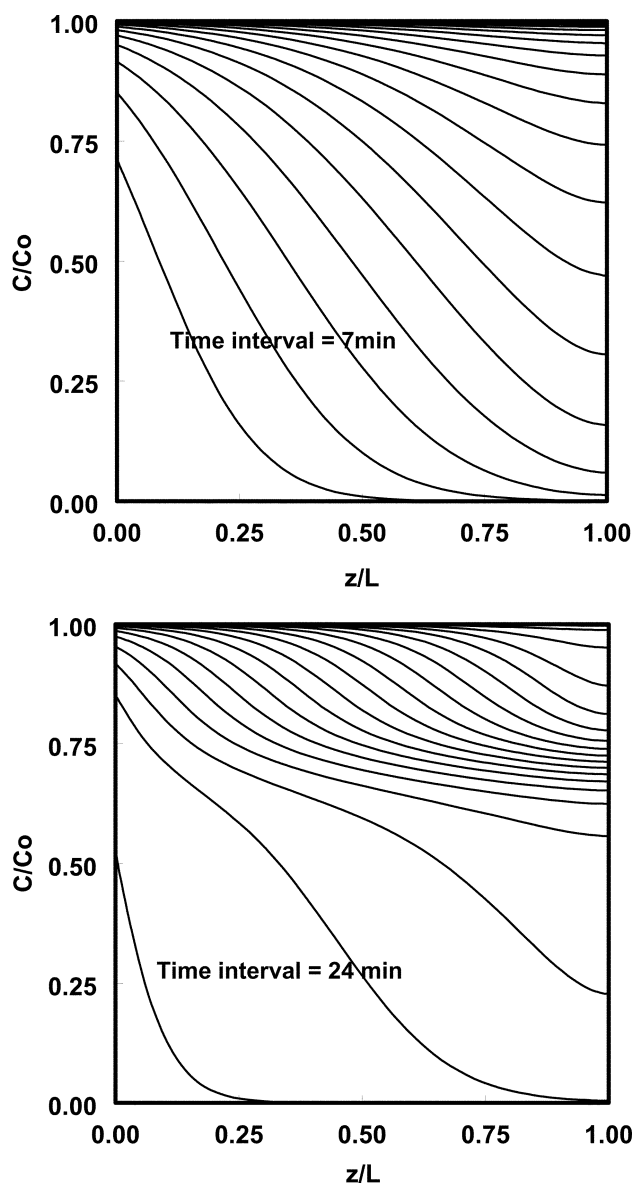


Fig. 9. Concentration profiles of TCE on MCM-48 pellet in the bed at 1.76 kPa (top) and 5.07 kPa (bottom).

as the adsorption step, since it requires a great deal of energy. Fig. 10 shows the effects of several temperatures on desorption profiles of the adsorber saturated with TCE at a partial pressure of about 5.07 kPa. The desorption profile is similar to that of the adsorption curve that shows the plateau at the same temperature. With increasing regeneration temperature, the length of plateau was shortened gradually and the desorption time required was decreased greatly.

### CONCLUSIONS

In order to quantitatively analyze the unusual adsorption breakthrough curves, experimental and theoretical studies were carried out for the adsorption of TCE on the synthesized MCM-48. The adsorption data in the powder and pelletized MCM-48 were measured by using a quartz spring balance equipped in a high vacuum system and were well fitted with a temperature-dependent hybrid

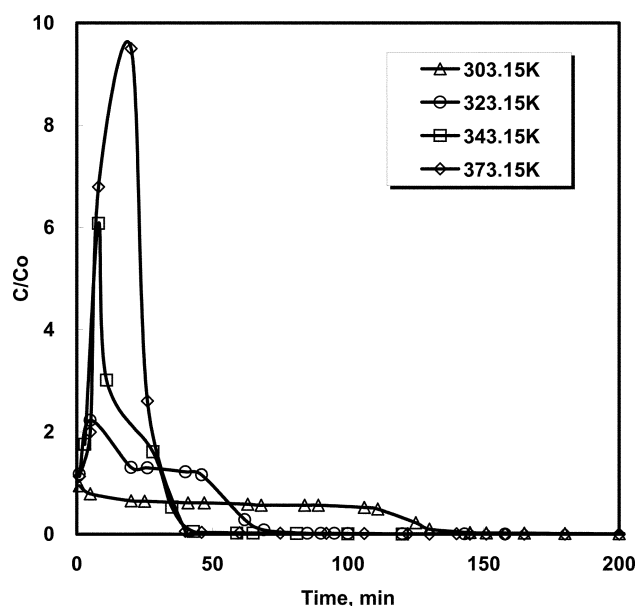


Fig. 10. Desorption breakthrough curves of TCE on MCM-48 pellet with respect to temperature.

isotherm equation. The temperature-dependent hybrid isotherm model is very useful for the correlation of solvent vapor adsorption on mesoporous adsorbents. Furthermore, the isosteric heat of adsorption was evaluated from the hybrid equation based on the Clausius-Clapeyron equation. The simple mathematical model employed in this study satisfactorily simulates the behavior of the adsorption breakthrough curve. This study will be valuable in design, simulation and optimization of adsorption-based processes for VOC removal by using mesoporous materials.

### ACKNOWLEDGMENT

This work was supported by grant No. (R-01-2001-00414-0 (2003)) from the Korea Science & Engineering Foundation.

### NOMENCLATURE

$b_1$	: hybrid isotherm parameter
$b_2$	: hybrid isotherm parameter
$c$	: bulk phase concentration [ $\text{mol}/\text{m}^3$ ]
$c_o$	: concentration of adsorbate in feed [ $\text{mol}/\text{m}^3$ ]
$D_e$	: effective diffusivity [ $\text{m}^2/\text{s}$ ]
$D_m$	: molecular diffusivity [ $\text{m}^2/\text{s}$ ]
$R_p$	: particle radius [m]
$D_L$	: axial dispersion coefficient in a fixed bed [ $\text{m}^2/\text{s}$ ]
$k_s$	: LDF mass transfer coefficient [ $\text{s}^{-1}$ ]
$k_f$	: external film mass transfer coefficient [m/s]
$L$	: bed length [m]
$n$	: hybrid isotherm parameter
$q$	: amount adsorbed [mol/kg]
$q_m$	: hybrid isotherm parameter
$q_{st}$	: isosteric heat of adsorption [kJ/mol]
$R$	: gas constant (=8.3143 J/mol·K)
$T$	: time [s]

T : temperature [K]  
 Z : axial position [L]

### Greek Letters

$\epsilon_B$  : bed porosity  
 $\epsilon_p$  : particle porosity  
 $\rho_g$  : bulk density of adsorbent particles in a fixed bed [kg/m<sup>3</sup>]  
 $\rho_p$  : particle density of adsorbent particles [kg/m<sup>3</sup>]  
 $v$  : interstitial velocity [m/s]

### Abbreviations

Re : Reynolds number  
 Sc : Schmidt number  
 Sh : Sherwood number

## REFERENCES

- Brown, P. N., Byrne, G. D. and Hindmarsh, A. C., "VODE: A Variable Coefficient ODE Solver," *SIAM J. Sci. Stat. Comput.*, **10**, 1038 (1989).
- Cho, S. Y., Jeong, S. J., Kim, S. J. and Chun, H. S., "Adsorption Equilibria Characteristics of Some Chlorinated Cleaning Solvent Vapors," *Korean J. Chem. Eng.*, **20**, 387 (2003).
- Corma, A., "From Microporous to Mesoporous Molecular Sieve Materials and Their Use in Catalysis," *Chem Rev.*, **97**, 2373 (1997).
- Farooq, S. and Ruthven, D. M., "Heat Effects in Adsorption Column Dynamics: 2. Experimental Validation of the One-Dimensional Model," *Ind. Eng. Chem. Res.*, **29**, 1084 (1990).
- Edwards, M. F. and Richardson, J. F., "Gas Dispersion in Packed Bed," *Chem. Eng. Sci.*, **23**, 109 (1968).
- Fuller, E. N., Schettler, P. D. and Giddings, J. C., "A Comparison of Methods for Predicting Gaseous Diffusion Coefficients," *J. Gas Chromatography*, **3**, 222 (1965).
- Gregg, S. J. and Sing, K. S. W., "Adsorption, Surface Area and Porosity," Academic Press, New York (1982).
- Hartmann, M. and Bishof, C., "Mechanical Stability of Mesoporous Molecular Sieve MCM-48 Studied by Adsorption of Benzene, n-Heptane, and Cyclohexane," *J. Phys. Chem. B*, **103**, 6230 (1999).
- Hill, T. L., "Statistical Mechanics of Adsorption. V. Thermodynamics and Heat of Adsorption," *J. Chem. Phys.*, **17**, 520 (1949).
- Hwang, K. S., Choi, D. K., Gong, S. Y. and Cho, S. Y., "Adsorption and Thermal Regeneration of Methylene Chloride Vapor on an Activated Carbon Bed," *Chem. Eng. Sci.*, **52**, 1111 (1997).
- Khan, F. I. and Ghoshal, A. K., "Removal of Volatile Organic Compounds from Polluted Air," *J. Loss. Prevent. Proc.*, **13**(6), 527 (2000).
- Kim, S. J., Cho, S. Y. and Kim, T. Y., "Adsorption of Chlorinated Volatile Organic Compounds in a Fixed Bed of Activated Carbon," *Korean J. Chem. Eng.*, **19**, 61 (2002).
- Lee, J. W., Lee, J. W., Shim, W. G., Suh, S. H. and Moon, H., "Adsorption of Chlorinated Volatile Organic Compounds on MCM-48," *J. Chem. Eng. Data*, **48**, 381 (2003).
- Lee, J. W., Shim, W. G. and Moon, H., "Adsorption Equilibrium and Kinetics for Capillary Condensation of Trichloroethylene on MCM-41 and MCM-48," *Micropor. Mesopor. Mat.*, submitted (2003).
- Malek, A. and Farooq, S., "Comparison of Isotherm Models for Hydrocarbon Adsorption on Activated Carbon," *AIChE J.*, **42**(11), 3191 (1996).
- Malek, A. and Farooq, S., "Kinetics of Hydrocarbon Adsorption on Activated Carbon and Silica Gel," *AIChE J.*, **43**(3), 761 (1997).
- Oh, J. S., Shim, W. G., Lee, J. W., Kim, J. H., Moon, H. and Seo, G., "Adsorption Equilibrium of Water Vapor on Mesoporous Materials," *J. Chem. Eng. Data*, **48**(6), 1458 (2003).
- Park, I. and Knabel, K. S., "Adsorption Breakthrough Behavior: Unusual Effects and Possible Causes," *AIChE J.*, **38**(5), 660 (1992).
- Riggs, J. B., "An Introduction to Numerical Methods for Chemical Engineers," Texas Tech. University Press, Lubbock (1988).
- Ruddy, E. N. and Carroll, L. A., "Select the Best VOC Control Strategy," *Chem. Eng. Prog.*, **89**, 28 (1993).
- Shim, W. G., Lee, J. W., Lee, J. W. and Moon, H., "Adsorption Dynamics of CVOCs Vapor on MCM-48," Fourth International Symposium Effect of Surface Heterogeneity in Adsorption and Catalysis on Solids, Krakow, Poland (2001).
- Shim, W. G., Lee, J. W. and Moon, H., "Adsorption of Carbon Tetrachloride and Chloroform on Activated Carbon at (300.15, 310.15, 320.15, and 330.15) K," *J. Chem. Eng. Data*, **48**(2), 286 (2003a).
- Shim, W. G., Lee, J. W. and Moon, H., "Equilibrium and Fixed-Bed Adsorption of n-Hexane on Activated Carbon," *Sep. Sci. Tech.*, **38**(16), 3905 (2003b).
- Silva, J. A. and Rodrigues, A. E., "Fixed-Bed Adsorption of n-Pentane/Isopentane Mixtures in Pellets of 5A Zeolite," *Ind. Eng. Chem. Res.*, **36**, 3769 (1997).
- Sircar, S., "New Adsorption-Condensation Theory for Adsorption of Vapors on Porous Activated Carbons," *Carbon*, **25**, 39 (1987).
- U.S. Department of Health and Human Services, 9th Report on Carcinogens. <http://ehp.niehs.nih.gov/>
- Villadesen, J. V. and Stewart, W. E., "Solution of Boundary Value Problems by Orthogonal Collocation," *Chem. Eng. Sci.*, **22**, 1483 (1967).
- Yang, R. T., "Gas Separation by Adsorption Processes," Butterworths, Boston (1986).
- Yun, J. H., "Unusual Adsorber Dynamics Due to S-Shaped Equilibrium Isotherm," *Korean J. Chem. Eng.*, **17**, 613 (2000).
- Wakao, N. and Funazkri, T., "Effect of Fluid Dispersion Coefficients on Particle to Fluid Mass Transfer Coefficients in Packed Bed," *Chem. Eng. Sci.*, **33**, 1375 (1978).
- Zhao, X. S., Lu, G. Q. and Hu, X., "Organophilicity of MCM-41 Adsorbents Studied by Adsorption and Temperature-programmed Desorption," *Colloids Surf. A*, **179**, 261 (2001).